Faraday Discussions

Membrane Electrostatics Sensed by Tryptophan Anchors in Hydrophobic Model Peptides Depends on Non-Aromatic Interfacial Amino Acids: Implications in Hydrophobic Mismatch

Journal:	*Faraday Discussions*
Manuscript ID	FD-ART-05-2020-000065.R1
Article Type:	Paper
Date Submitted by the Author:	09-Sep-2020
Complete List of Authors:	Pal, Sreetama; Centre for Cellular and Molecular Biology CSIR; Indian Institute of Chemical Technology CSIR; Academy of Scientific and Innovative Research Koeppe II, Roger; University of Arkansas, Chemistry and Biochemistry Chattopadhyay, Amitabha; Centre for Cellular and Molecular Biology CSIR; Academy of Scientific and Innovative Research

Membrane Electrostatics Sensed by Tryptophan Anchors in Hydrophobic Model Peptides Depends on Non-Aromatic Interfacial Amino Acids: Implications in Hydrophobic Mismatch

Sreetama Pal,*[abc] Roger E. Koeppe II[d] and
Amitabha Chattopadhyay*[ac]

[a]CSIR-Centre for Cellular and Molecular Biology, Hyderabad 500 007, India; [b]CSIR-Indian Institute of Chemical Technology, Hyderabad 500 007, India; [c]Academy of Scientific and Innovative Research, Ghaziabad 201 002, India; [d]Department of Chemistry and Biochemistry, University of Arkansas, AR 72701, USA

*Address correspondence to Sreetama Pal (sreetama@ccmb.res.in) or
Amitabha Chattopadhyay (amit@ccmb.res.in)

[†]Electronic supplementary information (ESI) available: Section S1, preparation of unilamellar vesicles; Section S2, steady state fluorescence measurements; Section S3, time-resolved fluorescence measurements; Fig. S1, representative fluorescence emission spectra of WALP tryptophans showing the shift in emission maximum upon red edge excitation; Fig. S2, representative time-resolved fluorescence intensity decay profile of WALP tryptophans.

Abstract

WALPs are synthetic α-helical membrane-spanning peptides that constitute a well-studied system for exploring hydrophobic mismatch. These peptides represent a simplified consensus motif for transmembrane domains of intrinsic membrane proteins due to their hydrophobic core of alternating leucine and alanine flanked by membrane-anchoring aromatic tryptophan residues. Although the modulation of mismatch responses in WALPs by tryptophan anchors has been reported earlier, there have been limited attempts to utilize the intrinsic tryptophan fluorescence of this class of peptides as mismatch sensors. We have previously shown, utilizing the red edge excitation shift (REES) approach, that interfacial WALP tryptophan residues in fluid phase bilayers experience a dynamically constrained membrane microenvironment. Interestingly, emerging reports suggest the involvement of non-aromatic interfacially localized residues in modulating local structure and dynamics in WALP analogs. In this backdrop, we have explored the effect of interfacial amino acids, such as lysine (in KWALPs) and glycine (in GWALPs), on the tryptophan microenvironment of WALP analogs in zwitterionic and negatively charged membranes. We show that interfacial tryptophans in KWALP and GWALP experience a more restricted microenvironment, as reflected in the substantial increase in magnitude of REES and apparent rotational correlation time, relative to those in WALP in zwitterionic membranes. Interestingly, in contrast to WALP, tryptophan anchors in KWALP and GWALP appear insensitive to the presence of negatively charged lipids in the membrane. These results bring out a subtle interplay between non-aromatic flanking residues in transmembrane helices and negatively charged lipids at the membrane interface, which could modulate the membrane microenvironment experienced by interfacially localized tryptophan residues. Since interfacial tryptophans are known to influence mismatch responses in WALPs, our results point out the possibility of utilizing fluorescence signatures of tryptophans in membrane proteins or models peptides such as WALP as markers for assessing protein responses to hydrophobic mismatch. More importantly, these results constitute one of the first reports on the influence of lipid headgroup charge in fine-tuning hydrophobic mismatch in membrane

bilayers, thereby enriching the existing framework of hydrophobic mismatch.

1 Introduction

Membrane-mediated regulation of cellular responses could arise due to the interaction of membrane proteins with specific lipids, or the influence of global bilayer properties on conformational dynamics and partitioning of membrane proteins, or a combination of both.[1] The modulation of membrane protein function by the membrane bilayer has its genesis, in part, in the strong coupling of the protein hydrophobic core to the lipid membrane hydrophobic thickness.[2,3] This hydrophobic coupling, termed as the hydrophobic matching principle,[4] is implicated in membrane protein sorting, localization, stability, topology and function.[5-8] Unraveling the molecular basis and consequences of hydrophobic (mis)match at the protein-lipid interface requires a systematic exploration of the organization and dynamics of transmembrane domains of membrane proteins in the context of global properties of their immediate microenvironment.

The WALP class of peptides (acetyl-GWW$(LA)_n$LWWA-ethanolamide), synthesized based on gramicidin as a template, constitutes the most well-studied model system for hydrophobic mismatch. WALPs consist of a helical hydrophobic core, constructed from alternating alanine and leucine residues, capped at each end by aromatic amino acids, such as tryptophan (see Fig. 1a).[9] The terminal residues typically are unwound from the core helix.[10,11] These peptides, therefore, represent a consensus motif for transmembrane domains of intrinsic membrane proteins due to the leucine and alanine residues, which are characterized by a high propensity of adopting α-helical conformation. This model, albeit simplistic, is appropriate since transmembrane segments of integral membrane proteins consist of a primarily hydrophobic α-helical core, flanked at each end by aromatic and charged residues.[12-14] In addition, the number of alanine-leucine repeats in this class of peptides can be used as a handle to tune the hydrophobic length and subsequent response of these peptides to a wide spectrum of (positive or negative) hydrophobic mismatch.

WALPs have been shown to respond to hydrophobic mismatch conditions by inducing non-bilayer structures in model membranes[9,15] and *E. coli* membrane mimics.[16] The stabilization of non-lamellar membrane phases in the presence of WALPs has been ascribed

to the flanking tryptophan residues, which may override the commonly observed peptide response to mismatch conditions.[17] This suppression of peptide responses to mismatch conditions by interfacial tryptophan residues could be attributed to the preference of this amino acid for the membrane interface[14,18-20] and possibly originates from its participation in hydrogen bonding with lipid carbonyls and interfacial water molecules.[21] Due to the design and architecture of these peptides, including the interfacial anchoring, their responses to hydrophobic mismatch is manifested predominantly as changes in tilt angles[22-24] and helix rotations or helical distortions,[25] and are dictated by the nature of the interfacial residues.

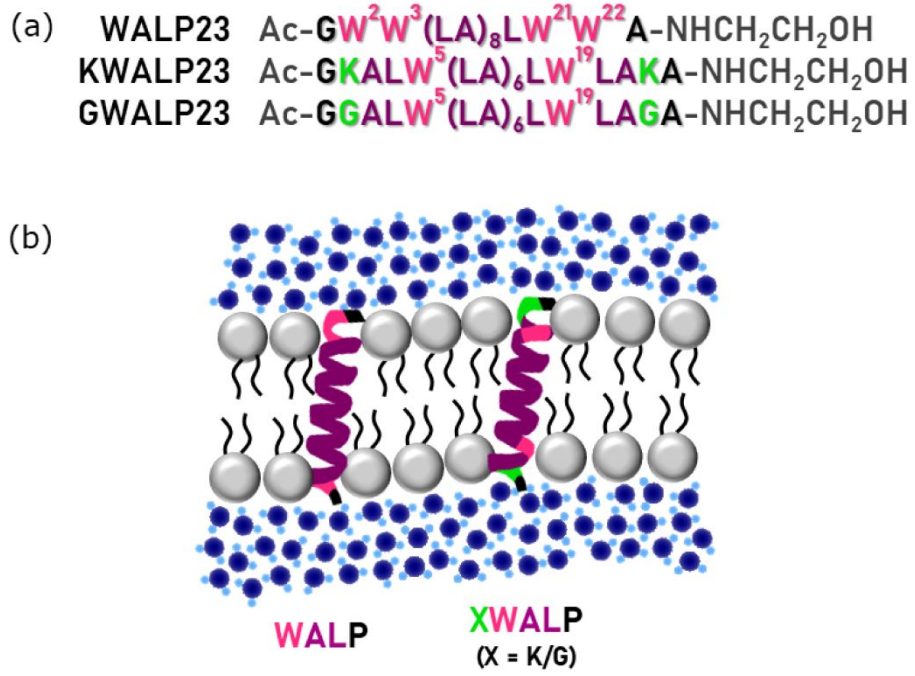

Fig. 1 A schematic showing the (a) amino acid sequence of the model transmembrane peptide WALP23 and its XWALP23 analogs, KWALP23 and GWALP23 (Ac represents acetyl group), and (b) membrane topology of these analogs. WALP analogs are a class of synthetic peptides that consist of a hydrophobic core of alternating alanine and leucine residues (shown in purple), capped on each side by aromatic amino acids such as tryptophan (marked in pink). This characteristic sequence ensures that WALP peptides represent a consensus sequence for α-helical transmembrane domains of membrane proteins. The XWALP (X = K/G) analogs represent variations of the prototypical WALP sequence, each with only one tryptophan anchor near each terminal and the other tryptophan on both termini replaced with lysine or glycine (shown in green). The hydrophobic length of the peptide can be tuned by changing the number of alanine-leucine repeats, thereby making these peptides excellent systems for exploring signatures and consequences of hydrophobic mismatch in membranes. The phospholipid headgroups are depicted as gray beads and fatty acyl chains are shown in black. Water molecules are depicted in shades of blue. See text for more details.

Despite studies highlighting the contribution of tryptophan anchors in modulating the membrane interaction of the WALP class of peptides, there have been very few attempts to explore this phenomenon utilizing the intrinsic fluorescence of these tryptophan residues. This issue assumes significance since interfacially localized tryptophan residues are indispensable in supporting membrane protein function and are known to define the protein hydrophobic length by acting as membrane anchors.[14] In this context, fluorescence readouts of interfacial tryptophans have emerged as sensitive markers for membrane protein organization, dynamics and function.[26-28] The restricted microenvironment experienced by tryptophan residues localized at the membrane interface has been shown to correlate with the function of several membrane-interacting peptides, including the ion channel peptide gramicidin[29,30] and the lytic peptide melittin.[31] In addition, hydrophobic mismatch experienced by gramicidin in membrane bilayers has been shown to manifest as changes in motional restrictions in the tryptophan microenvironment.[32]

We have previously shown, utilizing red edge excitation shift (REES), that interfacial WALP tryptophans experience a dynamically constrained membrane microenvironment.[33] Interestingly, emerging evidence suggests the involvement of interfacially localized non-aromatic amino acids in modulating local structure and dynamics in WALP analogs.[11,24] In this backdrop, we probed whether the distinct interfacial electrostatics imposed by zwitterionic and negatively charged membranes is sensed differentially by tryptophan residues in WALP analogs due to the presence of non-aromatic flanking residues such as lysine (in KWALP: (acetyl-GKALW$(LA)_{n-2}$LWLAKA-ethanolamide)) or glycine (in GWALP: (acetyl-GGALW$(LA)_{n-2}$LWLAGA-ethanolamide)). Our results suggest that non-aromatic flanking residues at the membrane interface indeed may contribute to membrane protein organization and function by modulating the extent to which tryptophan residues can sense their immediate microenvironment. These results point out the possible involvement of the membrane interface in modulating hydrophobic (mis)match response and could enrich the existing framework of hydrophobic mismatch. These observations assume significance in the overall backdrop of the well-documented role of tryptophan residues in shaping membrane protein structure and function,[14,29-31,34] and in the specific context of tryptophan-mediated

protein response to hydrophobic mismatch in membranes.[19]

2 Experimental

2.1 Materials

1-Palmitoyl-2-oleoyl-*sn*-glycero-3-phosphocholine (POPC) and 1-palmitoyl-2-oleoyl-*sn*-glycero-3-phosphoglycerol (POPG) lipids were obtained from Avanti Polar Lipids (Alabaster, AL). WALP23, KWALP23 and GWALP23 peptides were synthesized as described previously.[9,24] Lipids were checked for purity by thin layer chromatography and phospholipid concentration was determined by phosphate assay, as described earlier.[33] Peptide concentration was calculated based on the tryptophan abundance, using a molar extinction coefficient (ε) of 22,400 $M^{-1}cm^{-1}$ for WALP and 11,200 $M^{-1}cm^{-1}$ for KWALP or GWALP at 280 nm.[35] Chemicals of the highest available purity, UV spectroscopy grade solvents, and water purified through a Millipore (Bedford, MA) Milli-Q system were used for all experiments.

2.2 Preparation of unilamellar vesicles

Unilamellar vesicles (ULVs) of POPC or POPC/POPG (70/30, mol/mol) containing 2 mol% of the peptide (WALP23 or KWALP23 or GWALP23) suspended in 10 mM sodium phosphate, 150 mM sodium chloride, pH 7.2 buffer were used for all experiments. The total amount of lipid and each peptide was kept constant at 550 and 11 nmol, respectively, which translates to a lipid/peptide ratio of 50 (mol/mol). ULVs were prepared by sonication using a Sonics Vibra-Cell VCX 500 sonifier (Sonics & Materials Inc, Newtown, CT) fitted with a titanium microtip, as described previously.[33] The protocol for ULV preparation is described in the ESI.† The final concentration of lipid and peptide in the ULVs were 550 and 11 μM, respectively. Background samples (without the peptide) were prepared in a similar manner. All experiments were carried out with at least three sets of samples at room temperature (~23 °C).

2.3 Steady state fluorescence measurements

Steady state fluorescence data were acquired in a Fluorolog-3 Model FL3-22 spectrofluorometer (Horiba Jobin Yvon, Edison, NJ) using semi-micro quartz cuvettes. Slit widths of 2 and 4 nm were used for excitation and emission, respectively. In each case, the reported emission maxima were identical to (or within ±1 nm of) the values reported. Fluorescence anisotropy data were acquired using the Glan-Thompson polarization accessory in the same setup, with the same slit width parameters. Details of the acquisition parameters are outlined in the ESI.†

2.4 Time-resolved fluorescence measurements

Time-resolved fluorescence intensity decays were recorded using a Delta-D TCSPC setup (Horiba Jobin Yvon IBH, Glasgow, UK) in the time-correlated single photon counting (TCSPC) mode, as described earlier.[36] A pulsed light-emitting diode (DD-290), with a typical pulse width of 0.8 ns, was used as an excitation source. The LED profile (reflecting the instrument response function (IRF)) was measured using colloidal silica (Ludox) as a scatterer. Data were collected, stored and analyzed using the in-built plugins in the EzTime software version 3.2.2.4 (Horiba Scientific, Edison, NJ). Fluorescence intensity decay curves were deconvoluted with the IRF and analyzed as a sum of exponential terms to yield pre-exponential factors and the corresponding fluorescence decay times. A fit was considered acceptable when plots of the weighted residuals and their autocorrelation function exhibited random deviation about zero, with a χ^2 value of not more than 1.2. The intensity-averaged mean fluorescence lifetime ($<\tau>$) was calculated from the values extracted for these decay parameters. Data reported is representative of at least three independent measurements. Further details of the data acquisition parameters and analysis are described in the ESI.†

2.5 Data analysis and plotting

Student's two-tailed unpaired *t*-test, performed using GraphPad Prism software version 4.0 (San Diego, CA), was used to check statistical significance of the data. Microcal

Origin version 8.0 (OriginLab, Northampton, MA) was used for all other data analysis and plotting.

3 Results

WALPs are prototypical α-helical transmembrane peptides that represent a consensus sequence for transmembrane domains of integral membrane proteins due to the presence of leucine-alanine repeats flanked by membrane-anchoring tryptophan residues at each end (Fig. 1a). These tryptophan residues ensure a transmembrane orientation of the peptide due to the stability associated with their interfacial localization,[14,19] even in mismatch conditions.[17] In this work, we have explored the organization and dynamics of interfacial tryptophan residues in WALP23 and its analogs (KWALP23 and GWALP23) in zwitterionic POPC and negatively charged POPC/POPG (70/30, mol/mol) ULVs utilizing the wavelength-selective fluorescence toolbox.[26,27,37] KWALP and GWALP represent variations of the prototypical WALP sequence, each with only one tryptophan anchor near each terminal, since the other tryptophan on both termini has been replaced with lysine or glycine.[24] We used POPC and POPC/POPG bilayers as model systems because the hydrophobic length of these bilayers in the fluid phase[38,39] is similar to the hydrophobic length of the transmembrane helix in WALP analogs (see Fig. 1b). The peptides utilized for the present work are known to adopt an α-helical conformation in a membrane milieu.[24,33]

Wavelength-selective fluorescence (which includes REES) represents a sensitive toolbox to assess the spectroscopic signature of polar fluorophores in motionally restricted microenvironments, such as membranes and proteins.[26,27,37,40] The phenomenon of REES is observed *only* if solvent relaxation in the immediate microenvironment of the fluorophore occurs at timescales slower than or comparable to fluorescence timescales. This leads to a temporal overlap of solvation dynamics with fluorophore dynamics in the excited state and allows us to utilize REES to explore the organization and dynamics of fluorophores at the membrane interface. Operationally, REES is defined as the magnitude of red shift in fluorescence emission maximum due to a concomitant shift in the excitation wavelength

toward the red edge. The magnitude of REES is proportional to the extent of restriction imposed on solvation dynamics in the vicinity of the fluorophore.

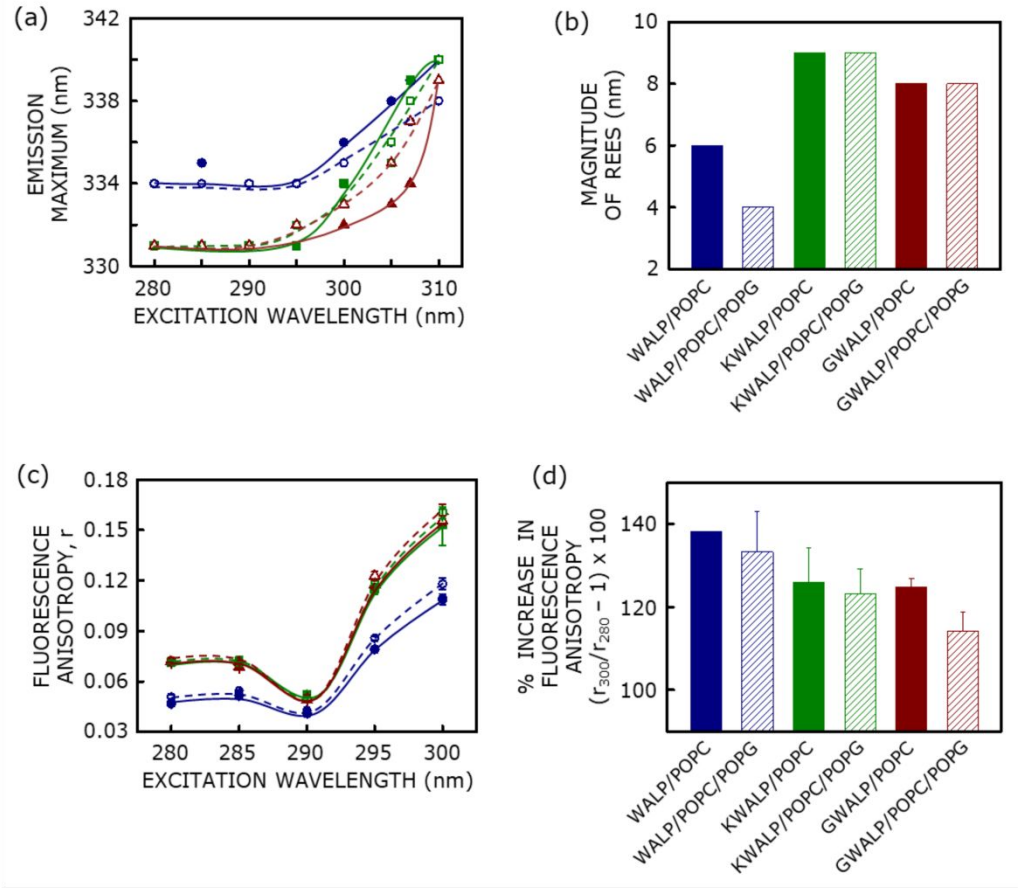

Fig. 2 Dependence of fluorescence emission maximum and anisotropy on excitation wavelength for WALP analogs in zwitterionic POPC and negatively charged POPC/POPG (70/30, mol/mol) membranes. (a) Red shift in emission maxima of WALP (●, blue), KWALP (■, green) and GWALP (▲, maroon) in POPC (filled symbols) and POPC/POPG (open symbols) membranes upon increasing the excitation wavelength. Data shown represent at least three independent measurements. Panel (b) shows the corresponding magnitude of REES, operationally defined as the shift in fluorescence emission maximum upon changing the excitation wavelength from 280 to 310 nm, for each WALP analog in POPC (filled bar) and POPC/POPG (hatched bar) membranes. (c) Increase in fluorescence anisotropy of tryptophan residues in WALP analogs with increasing excitation wavelength. The emission wavelength was kept constant at the emission maxima of each peptide obtained upon excitation at 280 nm, *i.e.*, 334 nm for WALP and 331 nm for KWALP/GWALP. Panel (d) shows the corresponding magnitude of increase in fluorescence anisotropy, calculated as the percentage increase in anisotropy at 300 nm relative to that at 280 nm. Data represent means ± SE of at least three independent measurements. Color-coding for panels (c) and (d) is the same as in panels (a) and (b), respectively. Lines joining the data points in panels (a) and (c) represent viewing guides. The concentration of each WALP analog was 11 μM and the lipid/peptide ratio was 50 (mol/mol) in all cases. See Experimental for more details.

The emission spectrum of WALP in POPC membranes displayed a characteristic maximum at 334 nm when excited at 280 nm (Fig. S1 in the ESI†), in agreement with our

previous results.[33] As shown in Fig. 2a, the emission maximum of WALP remained unchanged in POPC/POPG membranes. The shift in fluorescence emission maxima of the tryptophan residues of WALP analogs in POPC and POPC/POPG membranes with increasing excitation wavelength is also shown in Fig. 2a. For WALP in POPC membranes, the emission maximum exhibited a shift from 334 to 340 nm as the excitation wavelength was increased from 280 to 310 nm. This corresponds to REES of 6 nm (see Fig. 2b) and indicates that the interfacial WALP tryptophans in POPC membranes experience a microenvironment characterized by constrained solvation dynamics, consistent with our previous results.[33] Interestingly, the presence of negatively charged POPG lipids resulted in a REES of 4 nm (*i.e.*, 334 to 338 nm, see Fig. 2a) for WALP, implying a reduction in the constrained dynamics experienced by WALP tryptophans. A similar effect of interfacial membrane electrostatics on tryptophan organization and dynamics using REES has been previously reported.[31]

The corresponding REES data for WALP analogs KWALP and GWALP are shown in Figs. 2a and b. The emission maximum of KWALP in POPC was observed at 331 nm upon excitation at 280 nm. This got shifted to 340 nm upon red edge excitation at 310 nm, resulting in a REES of 9 nm (Fig. 2b). The magnitude of REES for KWALP was therefore higher relative to that of WALP in POPC membranes, implying increased motional restriction in the fluorophore microenvironment. Interestingly, the observed emission maximum (331 nm) and REES (9 nm) of KWALP in anionic POPC/POPG membranes turned out to be the same as that observed in zwitterionic POPC membranes. In other words, the fluorescence spectral signatures of KWALP appear to lack sensitivity to lipid composition and membrane interfacial electrostatics. In case of GWALP, the emission maximum in POPC membranes was found to be at 331 nm when excitation was carried out at 280 nm. Upon increasing the excitation wavelength to 310 nm, the emission maximum was shifted to 339 nm, giving rise to REES of 8 nm in POPC membranes (Fig. 2b). The motional constraint of GWALP tryptophans in POPC membranes, therefore, appears to be more than that experienced by WALP tryptophans. Even in this case, the observed emission maximum (331 nm) and REES (8 nm) in anionic POPC/POPG membranes turned out to be identical to that

observed for GWALP in zwitterionic POPC membranes. Taken together, the influence of negatively charged lipids on tryptophan dynamics appears to be attenuated in KWALP and GWALP analogs, thereby suggesting that these flanking residues could be involved in modulating the immediate microenvironment of tryptophan residues at the membrane interface.

Fig. 2c shows that tryptophan fluorescence anisotropy, calculated using eqn (S1), exhibits increase with excitation wavelength in WALP analogs in zwitterionic and negatively charged membranes. The increase in fluorescence anisotropy (calculated as the percentage increase in anisotropy at 300 nm relative to that at 280 nm) is plotted in Fig. 2d. Fluorescence anisotropy was found to display a substantial change with increasing excitation wavelength, with a pronounced enhancement toward the red edge. Data from excitation wavelengths beyond 300 nm are not shown due to poor signal-to-noise ratio. Strong dipolar interactions of solvent-relaxed fluorophores (photoselected by excitation at the red edge) with the surrounding solvent molecules[37] would impose restrictions on tryptophan rotational dynamics, which is manifested as increase in fluorescence anisotropy. The initial dip in fluorescence anisotropy at ~290 nm shown in Fig. 2c is a spectroscopic signature of tryptophan residues in a restricted environment[37] and originates from complex tryptophan photophysics.[27,37,41]

Fig. 3a shows the dependence of mean fluorescence lifetime on emission wavelength for tryptophan residues in WALP analogs. A representative fluorescence decay profile of WALP tryptophans in POPC membranes is included as Fig. S2 in the ESI.[†] The intensity-averaged mean fluorescence lifetimes at different emission wavelengths were calculated using eqn (S3) and are shown in Tables 1-3. The increase in mean fluorescence lifetime (calculated as the percentage increase in fluorescence lifetime at 380 nm relative to that at 330 nm) of interfacial tryptophan residues in POPC and POPC/POPG membranes is shown in Fig. 3b. The increase in mean fluorescence lifetime with increasing emission wavelength could be explained as follows.[37,41] Emission at shorter wavelengths photoselects unrelaxed fluorophores with a dual mode of relaxation. This subpopulation relaxes both *via* fluorescence emission at the given excitation wavelength and decay to longer wavelengths,

although the latter remains unobserved due to the emission wavelength window chosen for data acquisition. These rapidly relaxing fluorophores photoselected at shorter emission wavelengths contribute to the shorter fluorescence lifetimes. In addition, fluorophore populations emitting at the red edge are subjected to greater extents of solvent relaxation (since they reside longer in the excited state) and therefore, exhibit higher fluorescence lifetime.

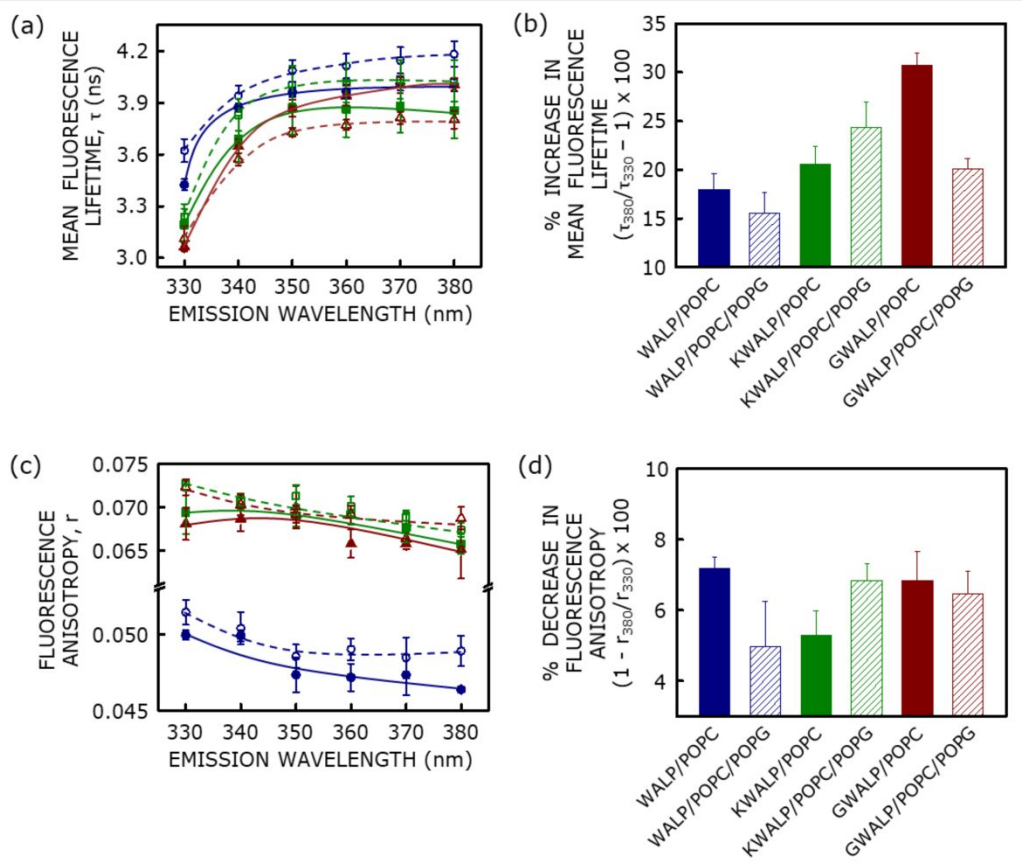

Fig. 3 Dependence of fluorescence lifetime and anisotropy on emission wavelength for WALP analogs in zwitterionic POPC and negatively charged POPC/POPG (70/30, mol/mol) membranes. (a) Effect of increasing emission wavelength on the intensity-averaged mean fluorescence lifetime of WALP (●, blue), KWALP (■, green) and GWALP (▲, maroon) in POPC (filled symbols) and POPC/POPG (open symbols) membranes. The excitation wavelength was 297 nm in all cases. Mean fluorescence lifetimes were calculated using eqn (S3). Panel (b) shows the corresponding magnitude of increase in mean fluorescence lifetime, calculated as the percentage increase in lifetime at 380 nm relative to that at 330 nm, for each WALP analog in POPC (filled bar) and POPC/POPG (hatched bar) membranes. (c) Reduction in fluorescence anisotropy of tryptophan residues in WALP analogs with increasing emission wavelength. Excitation wavelength was kept constant at 280 nm. Panel (d) shows the corresponding magnitude of decrease in fluorescence anisotropy, calculated as the percentage decrease in anisotropy at 380 nm relative to that at 330 nm. Data represent means ± SE of at least three independent measurements. Color-coding for panels (c) and (d) is the same as in panels (a) and (b), respectively. Lines joining the data points in panels (a) and (c) are viewing guides. The concentration of each WALP analog was 11 μM and the lipid/peptide ratio was 50 (mol/mol) in all cases. See Experimental for more details.

Fig. 3c shows the reduction in tryptophan fluorescence anisotropy in WALP analogs with increasing emission wavelength. The decrease in fluorescence anisotropy (calculated as the percentage decrease in anisotropy at 380 nm relative to that at 330 nm) in zwitterionic POPC and negatively charged POPC/POPG membranes is shown in Fig. 3d. Longer-lived fluorophores are photoselected at longer emission wavelengths. These fluorophores are characterized by lower values of fluorescence anisotropy at the red edge due to greater tumbling (rotation) in the excited state and subsequent depolarization. An additional factor complicating the wavelength-dependence of fluorescence anisotropy in WALP is the possibility of homo fluorescence resonance energy transfer (homo-FRET) due to the pairwise distribution of tryptophan residues at each end of WALP. This is due to a lack of orientational correlation between the photoselected donor and the subsequently excited acceptor involved in homo-FRET, which leads to fluorescence depolarization.[42,43] The lower values of tryptophan fluorescence anisotropy observed in WALP, relative to KWALP and GWALP peptides (Figs. 2c and 3c), lend credence to this possibility.

Since fluorescence anisotropy and lifetime represent sensitive parameters for monitoring the dynamics and environment of excited state fluorophores, an essential prerequisite for interpreting trends in fluorescence anisotropy is to ensure negligible interference from fluorescence lifetime induced artifacts. For this, apparent rotational correlation times were calculated using Perrin's equation:[44]

$$\tau_c = \frac{r \langle\tau\rangle}{r_o - r} \qquad (1)$$

where r_o is the fundamental anisotropy of tryptophan residues, r corresponds to fluorescence anisotropy (from Fig. 2c), and $\langle\tau\rangle$ is the mean fluorescence lifetime (from Tables 1-3). Fluorescence anisotropy and lifetime values obtained with excitation at 295 and 297 nm respectively, and emission wavelengths set to the corresponding emission maximum (*i.e.*, 334 nm for WALP and 331 nm for KWALP/GWALP) were used. The value of r_o was taken to be 0.16 for tryptophan residues.[45]

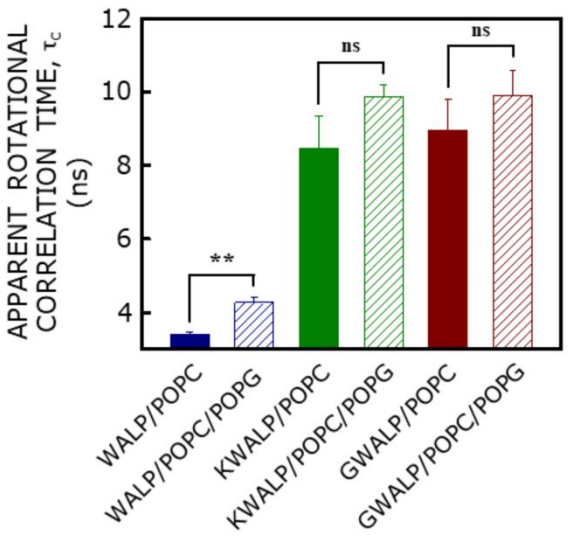

Fig. 4 Effect of the membrane microenvironment and non-aromatic flanking residues on the rotational dynamics of tryptophan in WALP analogs in zwitterionic POPC and negatively charged POPC/POPG (70/30, mol/mol) membranes. Apparent rotational correlation times of interfacial tryptophan residues in WALP (blue), KWALP (green) and GWALP (maroon) peptides embedded in POPC (filled bars) and POPC/POPG (hatched bars) membranes are shown. Apparent rotational correlation times were calculated using eqn (1) from fluorescence anisotropy values acquired with an excitation wavelength of 295 nm (data from Fig. 2c) and mean fluorescence lifetime recorded at an excitation of 297 nm (representative data shown in Tables 1-3). The emission wavelength for both fluorescence anisotropy and lifetime readouts was kept constant at the emission maxima of each peptide analog obtained upon excitation at 280 nm, *i.e.*, 334 nm for WALP and 331 nm for KWALP/GWALP. Data represent means ± SE of at least three independent measurements (** corresponds to significant ($p < 0.01$) difference in apparent rotational correlation time of WALP tryptophans in POPC/POPG membranes relative to that in POPC membranes and ns denotes statistically insignificant change). See Experimental and text for more details.

Fig. 4 shows the apparent (average) rotational correlation time of tryptophan residues in WALP analogs. In physical terms, rotational correlation time reflects the average time taken for a fluorophore (tryptophan, in this case) to rotate about its axis and is a reporter of order in the fluorophore microenvironment.[44] The rotational correlation time of WALP tryptophans in negatively charged POPC/POPG membranes was found to be significantly higher relative to that in zwitterionic POPC membranes. This indicates that interfacial WALP tryptophan residues in negatively charged membranes experience a more structured microenvironment, probably due to a higher fraction of ordered water molecules present at the membrane interface.[46,47] Interestingly, Fig. 4 shows that the rotational correlation time of tryptophan residues in KWALP/GWALP peptides in POPC membranes was significantly higher ($p < 0.01$, not shown) relative to WALP tryptophan residues. Therefore, the presence of non-aromatic interfacial flanking residues, such as lysine in KWALP and glycine in

GWALP, appears to result in slower rotational dynamics of interfacial tryptophan residues. Importantly, the rotational correlation times of KWALP and GWALP tryptophan residues remained invariant in the presence of negatively charged POPG lipids, thereby hinting at a subtle interplay of negatively charged lipids and non-aromatic flanking residues in modulating the microenvironment of interfacial tryptophan residues. These interpretations are reinforced by the trends observed in Figs. 2a and b.

4 Discussion

In this work, we have utilized the wavelength-selective fluorescence approach to explore the organization and dynamics of membrane-anchoring tryptophan residues in WALP and its analogs, KWALP and GWALP, in zwitterionic POPC and negatively charged POPC/POPG membranes. Our results reveal that tryptophans in all the WALP analogs exhibit REES, indicating that these aromatic residues are localized at or near the membrane interface and their microenvironment is characterized by restricted solvation dynamics. The presence of negatively charged lipids leads to a loss in motional restriction experienced by WALP tryptophans, as shown by a decrease in the magnitude of REES (see Fig. 2b). This change could be attributed to increased solvent exposure at the negatively charged membrane interface, as has been reported for other membrane-interacting peptides.[31] Nevertheless, the apparent rotational correlation time for WALP tryptophans exhibited an increase in the presence of negatively charged lipids. This is probably due to the presence of water molecules held in a more ordered collective network at the membrane interface by negatively charged lipids.[46,47] The apparently opposing trends in REES (Fig. 2a) and apparent rotational correlation times (Fig. 4) for WALP in negatively charged membranes relative to zwitterionic ones could have their origin in subtle difference in fluorophore properties represented by these observables. The wavelength-selective fluorescence approach reports predominantly on solvation dynamics in the fluorophore microenvironment, whereas apparent rotational correlation times reflect the restriction imposed on rotational dynamics of the fluorophore.

The restriction in solvation and rotational dynamics experienced by KWALP and GWALP tryptophan residues is significantly higher than that experienced by those in WALP (see Figs. 2b and 4). This restriction could be due to the presence of non-aromatic flanking residues such as lysine in KWALPs since lysine side chains are known to interact with the tryptophan indole ring *via* cation-π interactions.[48] The high motional restriction experienced by GWALP tryptophans could be a different effect, perhaps due to the greater tilt angle of GWALP relative to WALP (see Fig. 1b),[49] which would translate to deeper interfacial localization of GWALP tryptophan residues. Interestingly, tryptophan residues in KWALP and GWALP analogs appear to be insensitive to the lipid headgroup charge in negatively charged membranes, both with respect to solvation dynamics and apparent rotational correlation times (see Figs. 2b and 4). For KWALPs, cation-π-anion interactions[50] between lysine, tryptophan and negatively charged POPG could oppose the expected reduction in motional restriction of tryptophan microenvironment. This would result in dampening the influence of negatively charged lipids in tryptophan solvation and rotational dynamics, giving rise to invariant REES and apparent rotational correlation time for KWALP in zwitterionic and negatively charged membranes. In fact, electrostatic interactions between membrane lipids and proteins have been recently reported to complement the contribution of interfacial tryptophans toward stabilization of optimal (and functionally relevant) anchoring of transmembrane helices.[51] Taken together, these insights collectively point to the presence of novel and largely unexplored regulatory mechanisms at the helix-lipid interface, where a subtle interplay between non-aromatic flanking residues in transmembrane helices and negatively charged lipids could tune the microenvironment of interfacially localized tryptophan residues.

Membrane proteins (and peptides) are known to respond to hydrophobic mismatch in their immediate microenvironment by changing helical tilt angles,[6,8] which would correspond to changes in effective length of the hydrophobic core. In case of WALP analogs, the extent of helical tilt is coupled to the position of the tryptophan residues.[25,49] The fluorescence signatures of WALP tryptophans reported in this work could therefore be utilized as an indirect marker for helical tilt of transmembrane helices. In addition, judicious introduction

or repositioning of tryptophan residues in transmembrane domains of integral membrane proteins (represented by WALPs here) could induce not only differential tilt angles but also changes in dynamics and inter-helical packing of the transmembrane helix bundle.[52] This has important consequence for the modulation of membrane protein function by physicochemical aspects (including mismatch conditions) of the lipid microenvironment, since optimal helical tilt angles have been correlated to membrane protein stability and activity.[53-57] In particular, lysine could emerge as a key determinant in these local structural changes because these residues,[14] along with negatively charged lipids,[58] are known to be preferentially localized at the inner leaflet in biological membranes.

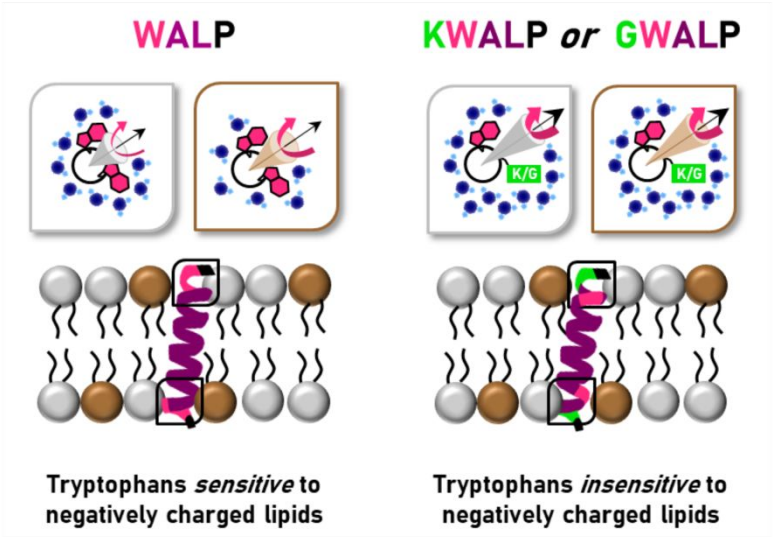

Fig. 5 Differential sensing of membrane interfacial electrostatics by tryptophan residues in WALP analogs due to the presence of non-aromatic flanking residues. Tryptophan residues are shown in pink, lysine/glycine in green, and leucine and alanine in purple. Phospholipids are depicted with gray (zwitterionic POPC) and brown (negatively charged POPG) headgroups, and black acyl chains. Schematic representations of the tryptophan microenvironment in WALP analogs in the presence of POPC (gray box) and POPG (brown box) are shown at the top. Dynamically constrained water molecules at the membrane interface are represented in shades of blue and reflect the extent of motional restriction experienced by the tryptophan residues. Fluorophore rotational dynamics is depicted with shaded cones and curly arrows, with the cones color coded to match the corresponding lipid headgroup. The left panel shows the decreased solvation dynamics (represented as lower number of slow relaxing interfacial water molecules) and increased apparent rotational correlation time (represented by increased size of the shaded cones and increased thickness of the pink curly arrow) characteristic of WALP tryptophans in the presence of POPG, relative to POPC. The right panel shows the significant difference in tryptophan microenvironment in KWALP and GWALP relative to that in WALP in POPC membranes. Tryptophan residues in KWALP and GWALP appear insensitive to the presence of negatively charged lipids (see text and Figs. 2b and 4). These insights collectively point to the presence of novel and largely unexplored regulatory mechanisms at the helix-lipid interface, where a subtle interplay between non-aromatic flanking residues in transmembrane helices and negatively charged lipids could tune the microenvironment of interfacially localized tryptophan residues. These results point out the involvement of membrane interfacial electrostatics in fine-tuning hydrophobic mismatch responses. See text for more details.

Taken together, our results suggest that non-aromatic residues, such as lysine and glycine, at the membrane interface could influence membrane protein stability, structure and function by modulating the extent to which tryptophan residues can sense their immediate microenvironment (Fig. 5). Since tryptophan interfacial localization has been shown to affect hydrophobic mismatch responses in WALP peptides,[17] the involvement of non-aromatic flanking residues in modulating tryptophan microenvironment could be expected to have important consequences for mismatch responses of transmembrane helical domains in membrane proteins. The current concept of hydrophobic mismatch is based primarily on the length of fatty acyl chains of membrane lipids, although the presence of cholesterol also can contribute.[8] Lipid acyl chains and cholesterol both are responsible for the mismatch between the hydrophobic core of the membrane and transmembrane domains of membrane peptides and proteins.[8] Our present results show that charge of the lipid headgroup could be an additional player in modulating hydrophobic mismatch in membranes. To the best of our knowledge, these results constitute one of the early reports on the involvement of membrane interfacial electrostatics in modulating hydrophobic mismatch responses. These observations assume significance in light of the crucial role of interfacial tryptophan residues in the organization, dynamics, topology and stability of several membrane-interacting peptides.[14,29-31,34] We envision that insights from our present results would enrich the prevalent framework of hydrophobic mismatch formalism and enhance our overall understanding of the importance of tryptophan localization, organization and dynamics in supporting membrane protein structure and function.

Conflict of Interest

There are no conflicts of interest to declare.

Acknowledgments

This work was supported by SERB Distinguished Fellowship grant (Department of Science and Technology, Govt. of India) to A.C. and core support from CSIR-Centre for Cellular and Molecular Biology. R.E.K. acknowledges support from MCB grant 1713242 from the United States National Science Foundation. S.P. thanks the University Grants Commission for the award of a Senior Research Fellowship. A.C. is a Distinguished Visiting Professor at the Indian Institute of Technology Bombay (Mumbai), and Adjunct Professor at Tata Institute of Fundamental Research (Mumbai) and Indian Institute of Science Education and Research (Kolkata), and an Honorary Professor at the Jawaharlal Nehru Centre for Advanced Scientific Research (Bengaluru). We thank G. Aditya Kumar for useful inputs in making some of the figures and members of the Chattopadhyay laboratory for their comments and discussions.

References

1. M. Jafurulla, G. A. Kumar, B. D. Rao and A. Chattopadhyay, *Adv. Exp. Med. Biol.*, 2019, **1115**, 21.
2. S. H. White and W. C. Wimley, *Biochim. Biophys. Acta*, 1998, **1376**, 339.
3. O. S. Andersen and R. E. Koeppe II, *Annu. Rev. Biophys. Biomol. Struct.*, 2007, **36**, 107.
4. O. G. Mouritsen and M. Bloom, *Biophys. J.*, 1984, **46**, 141.
5. M. S. Bretscher and S. Munro, *Science*, 1993, **261**, 1280.
6. J. A. Killian, *Biochim. Biophys. Acta*, 1998, **1376**, 401.
7. F. Dumas, M. C. Lebrun and J.-F. Tocanne, *FEBS Lett.*, 1999, **458**, 271.
8. B. D. Rao, S. Shrivastava and A. Chattopadhyay, in *Membrane Organization and Dynamics*, ed. A. Chattopadhyay, Springer, Heidelberg, 2017, 16, 375-387.
9. J. A. Killian, I. Salemink, M. R. R. de Planque, G. Lindblom, R. E. Koeppe II and D. V. Greathouse, *Biochemistry*, 1996, **35**, 1037.
10. A. Mortazavi, V. Rajagopalan, K. A. Sparks, D. V. Greathouse and R. E. Koeppe II, *ChemBioChem*, 2016, **17**, 462.
11. F. Afrose, M. J. McKay, A. Mortazavi, V. S. Kumar, D. V. Greathouse and R. E. Koeppe II, *Biochemistry*, 2019, **58**, 633.
12. I. T. Arkin and A. T. Brunger, *Biochim. Biophys. Acta*, 1998, **1429**, 113.
13. L. Adamian, V. Nanda, W. F. DeGrado and J. Liang, *Proteins*, 2005, **59**, 496.
14. D. A. Kelkar and A. Chattopadhyay, *J. Biosci.*, 2006, **31**, 297.
15. P. C. A. van der Wel, T. Pott, S. Morein, D. V. Greathouse, R. E. Koeppe II and J. A. Killian, *Biochemistry*, 2000, **39**, 3124.
16. S. Morein, R. E. Koeppe II, G. Lindblom, B. de Kruijff and J. A. Killian, *Biophys. J.*, 2000, **78**, 2475.
17. M. R. R. de Planque, B. B. Bonev, J. A. A. Demmers, D. V. Greathouse, R. E. Koeppe II, F. Separovic, A. Watts and J. A. Killian, *Biochemistry*, 2003, **42**, 5341.
18. J. A. Killian and G. von Heijne, *Trends Biochem. Sci.*, 2000, **25**, 429.
19. A. J. de Jesus and T. W. Allen, *Biochim. Biophys. Acta*, 2013, **1828**, 864.
20. R. E. Koeppe II, *J. Gen. Physiol.*, 2007, **130**, 223.
21. J. A. Ippolito, R. S. Alexander and D. W. Christianson, *J. Mol. Biol.*, 1990, **215**, 457.
22. E. Strandberg, S. Özdirekcan, D. T. S. Rijkers, P. C. A. van der Wel, R. E. Koeppe II, R. M. J. Liskamp and J. A. Killian, *Biophys. J.*, 2004, **86**, 3709.
23. S. Özdirekcan, D. T. S. Rijkers, R. M. J. Liskamp and J. A. Killian, *Biochemistry*, 2005, **44**, 1004.
24. V. V. Vostrikov, A. E. Daily, D. V. Greathouse and R. E. Koeppe II, *J. Biol. Chem.*, 2010, **285**, 31723.

25. A. E. Daily, D. V. Greathouse, P. C. A. van der Wel and R. E. Koeppe II, *Biophys. J.*, 2008, **94**, 480.
26. S. Haldar, A. Chaudhuri and A. Chattopadhyay, *J. Phys. Chem. B*, 2011, **115**, 5693.
27. A. Chattopadhyay and S. Haldar, *Acc. Chem. Res*., 2014, **47**, 12.
28. D. A. M. Catici, H. E. Amos, Y. Yang, J. M. H. van den Elsen and C. R. Pudney, *FEBS J.*, 2016, **283**, 2272.
29. S. S. Rawat, D. A. Kelkar and A. Chattopadhyay, *Biophys. J.*, 2004, **87**, 831.
30. A. Chattopadhyay, S. S. Rawat, D. V. Greathouse, D. A. Kelkar and R. E. Koeppe II, *Biophys. J.*, 2008, **95**, 166.
31. A. K. Ghosh, R. Rukmini and A. Chattopadhyay, *Biochemistry*, 1997, **36**, 14291.
32. D. A. Kelkar and A. Chattopadhyay, *Biochim. Biophys. Acta* 2007, **1768**, 2011.
33. S. Pal, R. E. Koeppe II and A. Chattopadhyay, *J. Fluoresc.*, 2018, **28**, 1317.
34. A. Chaudhuri, S. Haldar, H. Sun, R. E. Koeppe II and A. Chattopadhyay, *Biochim. Biophys. Acta*, 2014, **1838**, 419.
35. N. J. Gleason, V. V. Vostrikov, D. V. Greathouse, C. V. Grant, S. J. Opella and R. E. Koeppe II, *Biochemistry*, 2012, **51**, 2044.
36. S. Pal, R. Aute, P. Sarkar, S. Bose, M. V. Deshmukh and A. Chattopadhyay, *Biophys. Chem.*, 2018, **240**, 34.
37. S. Mukherjee and A. Chattopadhyay, *J. Fluoresc*., 1995, **5**, 237.
38. N. Kučerka, M.-P. Nieh and J. Katsaras, *Biochim. Biophys. Acta*, 2011, **1808**, 2761.
39. J. Pan, F. A. Heberle, S. Tristam-Nagle, M. Szymanski, M. Koepfinger, J. Katsaras and N. Kučerka, *Biochim. Biophys Acta*, 2012, **1818**, 2135.
40. A. P. Demchenko, *Methods Enzymol.*, 2008, **450**, 59.
41. S. Mukherjee and A. Chattopadhyay, *Biochemistry*, 1994, **33**, 5089.
42. F. T. S. Chan, C. F. Kaminski and G. S. K. Schierle, *ChemPhysChem*, 2011, **12**, 500.
43. S. Ganguly, A. H. A. Clayton and A. Chattopadhyay, *Biophys. J.*, 2011, **100**, 361.
44. J. R. Lakowicz, *Principles of Fluorescence Spectroscopy*, 3rd Ed, Springer, New York, 2006.
45. M. R. Eftink, L. A. Selvidge, P. R. Callis and A. A. Rehms, *J. Phys. Chem.*, 1990, **94**, 3469.
46. L. Janosi and A. A. Gorfe, *J. Chem. Theory Comput.* 2010, **6**, 3267.
47. S. Pal, N. Samanta, D. Das Mahanta, R. K. Mitra and A. Chattopadhyay, *J. Phys. Chem. B*, 2018, **122**, 5066.
48. D. A. Dougherty, *Acc. Chem. Res*., 2013, **46**, 885.
49. V. V. Vostrikov, C. V. Grant, A. E. Daily, S. J. Opella and R. E. Koeppe II, *J. Am. Chem. Soc.*, 2008, **130**, 12584.
50. D. Kim, E. C. Lee, K. S. Kim and P. Tarakeshwar, *J. Phys. Chem. A*, 2007, **111**, 7980.

51. A. J. Situ, S.-M. Kang, B. B. Frey, W. An, C. Kim and T. S. Ulmer, *J. Phys. Chem. B*, 2018, **122**, 1185.
52. M. J. McKay, A. N. Martfeld, A. A. De Angelis, S. J. Opella, D. V. Greathouse and R. E. Koeppe II, *Biophys. J.*, 2018, **114**, 2617.
53. J. Le Coutre, L. R. Narasimhan, C. K. N. Patel and H. R. Kaback, *Proc. Natl. Acad. Sci. USA*, 1997, **94**, 10167.
54. C.-S. Chiang, L. Shirinian and S. Sukharev, *Biochemistry*, 2005, **44**, 12589.
55. J. E. Donald, Y. Zhang, G. Fiorin, V. Carnevale, D. R. Slochower, F. Gai, M. L. Klein and W. F. DeGrado, *Proc. Natl. Acad. Sci. USA*, 2011, **108**, 3958.
56. F. Hilbers, W. Kopec, T. J. Isaksen, T. H. Holm, K. Lykke-Hartmann, P. Nissen, H. Khandelia and H. Poulsen, *Sci. Rep.*, 2016, **6**, 20442.
57. Z. Ren, P. X. Ren, R. Balusu and X. Yang, *Sci. Rep.*, 2016, **6**, 34129.
58. G. van Meer and A. I. P. M. de Kroon, *J. Cell Sci.*, 2011, **124**, 5.

Table 1

Representative mean intensity-averaged fluorescence lifetimes of WALP tryptophan residues in POPC and POPC/POPG membranes[a]

Emission wavelength (nm)	α_1	τ_1 (ns)	α_2	τ_2 (ns)	α_3	τ_3 (ns)	$\langle\tau\rangle$[b] (ns)	χ^2
POPC membranes								
330	0.17	1.73	0.12	5.00	0.71	0.19	3.43	1.16
334[c]	0.21	1.91	0.16	5.03	0.63	0.24	3.57	1.03
340	0.44	2.07	0.29	5.35	0.27	0.87	3.85	1.10
350	0.41	2.31	0.33	5.26	0.26	0.81	3.97	1.04
360	0.45	2.11	0.34	5.23	0.21	0.59	3.99	1.10
370	0.42	2.42	0.32	5.39	0.26	0.80	4.04	1.16
380	0.44	2.29	0.31	5.39	0.25	0.63	4.02	1.03
POPC/POPG membranes								
330	0.27	2.00	0.20	5.04	0.53	0.33	3.61	1.12
334[c]	0.34	1.99	0.23	5.12	0.43	0.33	3.72	1.06
340	0.35	2.19	0.30	5.21	0.35	0.35	4.02	1.15
350	0.42	2.56	0.32	5.35	0.26	0.87	4.02	1.09
360	0.44	2.39	0.34	5.33	0.22	0.73	4.06	1.11
370	0.44	2.72	0.32	5.47	0.24	1.00	4.10	1.10
380	0.42	3.01	0.29	5.67	0.29	1.24	4.15	1.07

[a]The excitation wavelength was 297 nm. A total of 10,000 photons were collected at the peak channel for robust data acquisition. The concentration of WALP was 11 μM and the lipid/peptide ratio was 50 (mol/mol). See Experimental for more details.

[b]Calculated using eqn (S3)

[c]Emission maximum

Table 2

Representative mean intensity-averaged fluorescence lifetimes of KWALP tryptophan residues in POPC and POPC/POPG membranes[a]

Emission wavelength (nm)	α_1	τ_1 (ns)	α_2	τ_2 (ns)	α_3	τ_3 (ns)	$\langle\tau\rangle$[b] (ns)	χ^2
POPC membranes								
330	0.09	1.75	0.09	4.76	0.82	0.18	3.19	1.06
331[c]	0.05	1.80	0.05	4.86	0.90	0.09	3.26	1.04
340	0.31	2.04	0.25	5.04	0.44	0.36	3.75	1.10
350	0.38	2.13	0.36	5.03	0.26	0.71	3.91	1.08
360	0.41	2.08	0.31	5.13	0.28	0.42	3.90	1.10
370	0.39	2.11	0.37	5.06	0.24	0.89	3.92	1.09
380	0.39	2.55	0.29	5.35	0.32	1.05	3.88	1.07
POPC/POPG membranes								
330	0.08	1.84	0.07	4.78	0.85	0.11	3.27	1.07
331[c]	0.13	1.90	0.11	4.80	0.76	0.16	3.37	1.16
340	0.21	2.08	0.28	4.94	0.51	0.26	3.98	1.12
350	0.42	2.02	0.38	4.91	0.20	0.74	3.84	1.05
360	0.31	2.34	0.35	5.18	0.34	0.29	4.22	1.08
370	0.31	2.30	0.35	5.11	0.34	0.27	4.17	1.11
380	0.45	2.61	0.34	5.46	0.21	0.54	4.22	1.10

[a]The excitation wavelength was 297 nm. A total of 10,000 photons were collected at the peak channel for robust data acquisition. The concentration of KWALP was 11 μM and the lipid/peptide ratio was 50 (mol/mol). See Experimental for more details.

[b]Calculated using eqn (S3)

[c]Emission maximum

Table 3

Representative mean intensity-averaged fluorescence lifetimes of GWALP tryptophan residues in POPC and POPC/POPG membranes[a]

Emission wavelength (nm)	α_1	τ_1 (ns)	α_2	τ_2 (ns)	α_3	τ_3 (ns)	$\langle\tau\rangle$[b] (ns)	χ^2
POPC membranes								
330	0.10	1.75	0.07	4.77	0.83	0.14	3.06	1.06
331[c]	0.15	1.83	0.10	4.91	0.75	0.20	3.21	1.12
340	0.32	2.08	0.23	5.10	0.45	0.37	3.70	1.07
350	0.43	2.36	0.30	5.28	0.27	0.78	3.89	1.11
360	0.43	2.43	0.30	5.37	0.27	0.87	3.94	1.13
370	0.43	2.27	0.32	5.31	0.25	0.77	3.97	1.09
380	0.41	2.54	0.29	5.51	0.30	0.97	4.00	1.07
POPC/POPG membranes								
330	0.13	1.89	0.08	5.01	0.79	0.21	3.09	1.09
331[c]	0.18	1.79	0.12	4.77	0.70	0.21	3.20	1.05
340	0.41	2.07	0.25	5.05	0.34	0.61	3.56	1.05
350	0.47	2.05	0.27	5.27	0.26	0.69	3.74	1.05
360	0.31	2.93	0.22	5.63	0.47	1.31	3.78	1.13
370	0.35	2.64	0.26	5.39	0.39	1.17	3.78	1.05
380	0.48	2.10	0.27	5.32	0.25	0.70	3.77	1.04

[a]The excitation wavelength was 297 nm. A total of 10,000 photons were collected at the peak channel for robust data acquisition. The concentration of GWALP was 11 μM and the lipid/peptide ratio was 50 (mol/mol). See Experimental for more details.

[b]Calculated using eqn (S3)

[c]Emission maximum